Treatment with the neutralizing antibody against repulsive guidance molecule-a promotes recovery from impaired manual dexterity in a primate model of spinal cord injury

Authors: Hiroshi Nakagawa[1,2]*, Taihei Ninomiya[1], Toshihide Yamashita[2], Masahiko Takada[1]

Affiliations:

[1]Systems Neuroscience Section, Primate Research Institute, Kyoto University, Inuyama, Aichi 484-8506, Japan.

[2]Department of Molecular Neuroscience, Graduate School of Medicine, Osaka University, Suita, Osaka 565-0871, Japan.

*Corresponding author: Hiroshi Nakagawa

Present address for HN: Sobell Department of Motor Neuroscience and Movement Disorders, Institute of Neurology, University College London, Queen Square, London, WN1C 3BG, United Kingdom. Tel: 44-20-3448-4403; Fax: 44-20-7813-3107; E-mail: h.nakagawa@ucl.ac.uk

Present address for TN: Department of System Neuroscience, National Institute for Physiological Sciences, 38 Nishigonaka Myodaiji, Okazaki, Aichi, 444-8585, Japan.

Running title: RGMa is a potential molecular target for SCI.

Keywords

manual dexterity; corticospinal tract; repulsive guidance molecule-a; primates; spinal cord injury

Abstract

Axons in the mature mammalian central nervous system have only a limited capacity to grow/regenerate after injury, and, therefore, spontaneous recovery of motor functions is not greatly expected in spinal cord injury (SCI). To promote functional recovery after SCI, it is critical that corticospinal tract (CST) fibers reconnect properly with target spinal neurons through enhanced axonal growth/regeneration. Here, we applied antibody treatment against repulsive guidance molecule-a (RGMa) to a monkey model of SCI. We found that inhibition of upregulated RGMa around the lesioned site in the cervical cord resulted in recovery from impaired manual dexterity by accentuated penetration of CST fibers into laminae VII and IX where spinal interneurons and motoneurons are located, respectively. Furthermore, pharmacological inactivation following intracortical microstimulation revealed that the contralesional, but not the ipsilesional, primary motor cortex was crucially involved in functional recovery at a late stage in our SCI model. The present data indicate that treatment with the neutralizing antibody against RGMa after SCI is a potential target for achieving restored manual dexterity in primates.

Introduction

Manual dexterity as represented by a precision grip is skilled motor behavior characteristic of higher primates. It is generally accepted that manual dexterity is closely related to direct connectivity of the corticospinal tract (CST) arising from the motor cortex to motoneurons of the cervical cord that control the distal hand muscles (Lemon, 1993). The spinal cord injury (SCI) disrupts the CST and often causes an ever-lasting disability with sensorimotor dysfunctions. Therefore, the CST has been focused as an essential target for SCI treatment (GrandPré et al., 2002; Oudega and Perez, 2012). However, the mature mammalian central nervous system (CNS) has only a limited capacity to grow/regenerate once injured because of a number of inhibitory factors, including axon guidance molecules (Yiu and He, 2006).

Repulsive guidance molecule-a (RGMa) is among the axon guidance molecules. This molecule was originally identified in the visual system (Stahl et al., 1990; Monnier et al., 2002), and has been implicated in neuronal survival, proliferation and differentiation (Matsunaga et al., 2004; Matsunaga et al., 2006; Lah and Key, 2012). RGMa was upregulated around the lesioned site after SCI in rodents (Schwab et al., 2005), and treatment with the neutralizing antibody against RGMa has been shown to accelerate axonal regrowth and sprouting from the CST following thoracic cord lesions

(Hata et al., 2006). On the other hand, to promote functional recovery by enhanced sprouting of CST fibers after CNS insults, such fibers are required to extend toward an appropriate locus and reconnect properly with target spinal neurons (Wahl et al., 2014). It has recently been reported in macaque monkeys that a number of sprouting CST fibers derived from the contralesional primary motor cortex (MI) after SCI penetrate, below the lesioned site, into laminae VII and IX where spinal interneurons and motoneurons are located, respectively. Moreover, the ratio of the axonal distribution was significantly increased in lamina IX (Nakagawa et al., 2015). By contrast, the sprouting CST fibers chiefly terminate within the medial gray matter in rodents (Hata et al., 2006; Vavrek et al., 2006). These results suggest that the mechanisms underlying axonal remodeling that leads to the recovery of motor functions after SCI may differ in higher primates and rodents. Therefore, it is important to understand axonal remodeling specific to higher primates for restoration of manual dexterity after SCI. It is also crucial to confirm whether RGMa suppression promotes the recovery from impaired manual dexterity for applying to human patients with SCI.

The present study aimed at establishing the antibody treatment against RGMa in higher primates. Our results indicate that treatment with the neutralizing antibody against RGMa is critical to achieve restored manual dexterity after SCI.

Materials and Methods

Animals

Twelve rhesus monkeys (*Macaca mulatta*, 3–5 years old, 3.8–5.4 kg) of either sex were used in the present study: three lesioned monkeys for treatment with control antibody (Ctrl-A to Ctrl-C), four monkeys for treatment with anti-RGMa antibody (RGMa-A to RGMa-D), and five normal monkeys for molecular biological (western blotting) and histological (histochemical, immunohistochemical, and *in situ* hybridization) analyses. The experimental protocols were approved by the Animal Welfare and Animal Care Committee of the Primate Research Institute, Kyoto University, Japan. All experiments were conducted in accordance with the Guide for Care and Use of Laboratory Primates (Ver. 3, 2010) by the Primate Research Institute, Kyoto University, Japan.

Anti-RGMa antibody

We used an anti-human RGMa antibody (mouse IgG; IBL) as a neutralizing antibody against RGMa in the present study. The antibody was raised against the C-terminal sequences of human RGMa, LYERTRDLPGRAAAGL. The protein sequence of human RGMa fully corresponds with that for macaque monkeys. It has

previously been reported that the antibody has an inhibitory effect on human RGMa obtained from peripheral blood mononuclear cells of human patients with multiple sclerosis (Muramatsu et al., 2011).

Western blotting

Following sedation with ketamine hydrochloride (10 mg/kg, i.m.) and xylazine hydrochloride (1 mg/kg, i.m.), an intact monkey was anesthetized deeply with sodium pentobarbital (50 mg/kg, i.v.) and perfused transcardially with 0.1 M phosphate-buffered saline (PBS; pH 7.4). The MI (digit region) and the spinal cord (C7 to Th1 segments) were harvested and homogenized in a lysis buffer, comprising 50 mM Tris-HCl (pH 7.8) with 150 mM NaCl, 1 mM EDTA, 2 mM Na_3VO_4, 1% NP-40, and protease inhibitor cocktail. After centrifugation at 13,000 g for 20 min at 4˚C, it was lysed by using equal amounts of 2 x sample buffer, comprising 250 mM Tris-HCl, 4% sodium dodecyl sulphate, 20% glycerol, 0.02% bromophenol blue, and 5% β-mercaptoethanol, and then proteins were boiled for 5 min at 95˚C. The mixed proteins were separated on sodium dodecyl sulphate polyacrylamide gel electrophoresis and transferred to a polyvinylidence fluoride membrane (Millipore). The membrane was blocked with 5% skim milk in 0.01 M PBS containing 0.05% Tween-20 and then

incubated with anti-RGMa antibody (IBL). After several washes, the membrane was incubated with horseradish peroxidase-linked anti-mouse IgG antibody (1:5,000; Cell Signaling Technology). The detection was carried out with an ECL chemiluminescence system (GE Healthcare). As control samples, human- and mouse-recombinant RGMa proteins (R & D systems) were used.

Experimental time-course

The experimental time-course was summarized in Figure 1N. The monkeys were trained with the two behavioral tasks, a reaching/grasping task and a modified Brinkman board test (Freund et al., 2006, 2009) for 2–3 months prior to SCI. To reduce the inter-animal variability in the modified Brinkman board test, pairs of monkeys who exhibited similar baselines before SCI (i.e., Ctrl-A and RGMa-A, Ctrl-B and RGMa-B, and Ctrol-C and RGMa-C) usually underwent simultaneous behavioral analyses. After SCI, the two behavioral tasks were performed to assess the extent of recovered forelimb movements over 14 weeks. Following all behavioral analyses, the digit regions of the contralesional and ipsilesional MI were identified in the anti-RGMa antibody-treated monkeys using intracortical microstimulation (ICMS), and then muscimol was injected into the identified digit regions to inactivate neuronal activity therein. To examine

sprouting CST fibers below the lesioned site, biotinylated dextran amine (BDA) was injected into the contralesional MI seven weeks prior to sacrifice. To label spinal motoneurons through the median nerve on the SCI side, wheat germ agglutinin-conjugated horseradish peroxidase (WGA-HRP) was infused from the cut end of the nerve four days prior to sacrifice. One of the four monkeys (RGMa-B) who were treated with the anti-RGMa antibody was excluded from the electrophysiological/pharmacological and histological analyses, because this monkey was dead by unknown accident shortly after the behavioral analyses.

Behavioral analyses

We investigated whether RGMa inhibition with the antibody might promote the recovery from impaired manual dexterity after SCI. To assess the extent to which the skilled motor behavior was restored in our SCI model, the two behavioral tasks, a reaching/grasping task and a modified Brinkman board test were performed. These tasks were designed to take out pellets from vertical and horizontal slots. Each behavioral analysis was carried out on the 3rd, 5th, 7th, and 10th day after SCI, and then twice a week until the 14th week.

154 Reaching/grasping task

155 This task was performed to assess quantitatively the extent of recovery of
156 dexterous manual movements as previously described (Nakagawa et al., 2015). Briefly,
157 the monkeys were seated in a primate chair, and an acrylic board which consisted of
158 three vertical or horizontal slots was placed in front of the chair (Fig. 4A,B). Each slot
159 was filled with a small pellet (diameter, 9 mm). The monkeys reached for the vertical or
160 horizontal slots and attempted to pick up three pellets within 10 sec in each trial. We
161 analyzed how many pellets the monkeys successfully collected in each session (7 trials).
162 Data were expressed as the ratio of the number of collected pellets to the total number
163 per session (21 pellets; 3 pellets x 7 trials) in each of the vertical-slot and horizontal-slot
164 tasks.

165

166 Modified Brinkman board test

167 The Brinkman board test was originally created to assess manual dexterity after
168 SCI at the cervical cord level in macaque monkeys (Rouiller et al., 1998). Later, Freund
169 et al. (2006, 2009) have made a minor modification for analyzing the extent of
170 functional recovery from SCI, and named it “a modified Brinkman board test”. In the
171 present study, we applied this modified version. The monkeys were seated in a primate

chair, and the Brinkman board was placed on the chair. The Brinkman board (10 cm x 20 cm) was made of an acrylic board where a total of 50 slots (15 mm long x 8 mm wide x 6 mm deep), consisting of 25 vertical and 25 horizontal slots, were randomly located on the board (Fig. 4E). Each slot was filled with a food pellet (94 mg, banana or very berry flavor; Bioserve). In our modified Brinkman board test, each session consisted of 50 trials (25 trials for each of the vertical- and horizontal-slot tasks) to take out a total of 50 pellets, and a trial was considered to be successful when the monkey grasped a pellet and conveyed it to the mouth within 30 sec. On the other hand, a trial was counted as an error when the monkey failed to grasp a pellet or dropped it on the way to the mouth. The baseline value prior to SCI was represented as the mean of successful trials (maximum = 25) per session in each of the vertical- and horizontal-slot tasks that were performed 7 times (5 sessions per day). In each monkey, the analyzed data were evaluated as the number of successful trials per session in a daily test.

Surgical procedures for SCI

Surgical procedures for SCI were performed as previously described with minor modifications (Nakagawa et al., 2015). Briefly, the monkeys were sedated with a combination of ketamine hydrochloride (10 mg/kg, i.m.), xylazine hydrochloride (1

mg/kg, i.m.), and atropine (0.05 mg/kg, i.m.), and then anesthetized with sodium pentobarbital (25 mg/kg, i.v.). The monkeys who were monitored with percutaneous oxygen saturation, respiration rate, heart rate, blood pressure, body temperature, and electrocardiogram were stabilized in a stereotaxic frame. The skin and axial muscles were dissected at the level of the C2 to T1 segments under aseptic conditions. Subsequently, laminectomy of the C3 to C7 segments was performed, and the dura mater was cut unilaterally. After identification of the dorsal roots at the C6 and C7 levels, a border between the C6 and the C7 segment was lesioned with a surgical blade (No. 11) and a special needle (27G). The anti-RGMa antibody or control antibody (IgG from mouse serum; Sigma-Aldrich) was continuously delivered, via an osmotic pump (2ML4, Alzet) installed under the skin of the back, to the periphery of the lesioned site over four weeks immediately after SCI. Both the anti-RGMa and the control antibodies purified as IgGs were concentrated to 50 μg/kg/day in PBS. To estimate the extent of antibody infusion in the spinal cord, a 1% solution of Fast blue (Polysciences) was used instead of the antibody. To fix properly a catheter (11 cm long) attached to the osmotic pump, the top of the catheter was placed 5 mm above the lesioned site under the dura mater (intrathecal administration) following SCI, and the catheter was connected to the dura mater and surrounding muscles with surgical suture to keep the position during the

delivery of the antibody (Fig. 1K). Subsequently, spongel (Astellas) was located on the dura mater for hemostasis, and then the muscles and skin were sutured. Following the surgery, the monkeys were given an analgesic (Lepetan; Otsuka; i.m.; Indomethacin; Isei; oral, one week) and an antibiotic (Viccillin; Meiji Seika; i.m., 3–4 days). Four weeks later, the osmotic pump was removed from the back under general anesthesia (see above) and, then, checked to ensure that the whole amount of the antibody was certainly delivered up.

Intracortical microstimulation (ICMS)

Under general anesthesia with sodium pentobarbital (25 mg/kg, i.v.), two pipes made of polyether ether ketone were mounted in parallel over the frontal and occipital lobes for head fixation. After partial removal of the skull over the central sulcus under aseptic conditions, two rectangular plastic chambers (for the contralesional MI, 37 mm long x 42 mm wide x 15 mm deep; for the ipsilesional MI, 28 mm long x 32 mm wide x 20 mm deep) were attached to the exposed skull. Several days later, each monkey was seated in a primate chair with the head fixed in a stereotaxic frame attached to the chair. A glass-coated tungsten microelectrode (0.5–1.5 MΩ at 1 kHz; Alpha Omega) was penetrated perpendicularly into the contralesional or ipsilesional MI to identify the digit

226 region. Parameters of electrical stimulation were as follows: trains of 11 and 44 cathodal
227 pulses, 200-μsec duration at 333 Hz, current of less than 65 μA. Basically, movements
228 of the digits on the MI stimulation are easily elicited by short trains in a normal control
229 (Miyachi et al., 2005). However, as we could assume that the movement threshold for
230 ICMS might become higher after SCI, we used a 44-pulse train in addition to a 11-pulse
231 train. Evoked movements of the digits were carefully monitored by visual inspection
232 and muscle palpation.
233
234 **Muscimol injections**
235 To confirm whether compensatory pathways arising from the contralesional MI
236 might be involved in recovery from impaired manual dexterity in our SCI model, the
237 gamma-aminobutyric acid type A ($GABA_A$) receptor agonist, muscimol (1 μg/μl in
238 physiological saline, Sigma-Aldrich), was injected into the
239 electrophysiologically-identified digit region of the contralesional or ipsilesional MI
240 through a 10-μl Hamilton microsyringe following ICMS. At each of four loci, 3 μl of
241 muscimol was very slowly infused (Fig. 6A). Saline was injected into the same sites
242 using the same parameters as a control. After the muscimol or saline injections into the
243 MI digit region, skilled forelimb movements were assessed with the reaching/grasping

task (for horizontal slots). Data were expressed as the ratio of successfully collected pellets to the total per session.

Anterograde tract-tracing of CST fibers

CST fibers below the lesioned site arising from the contralesional MI were anterogradely labeled with biotinylated dextran amine (BDA; Invitrogen; 10,000 MW). The BDA injections into the contralesional MI were performed seven weeks prior to sacrifice as previously described (Nakagawa et al., 2015). Briefly, under general anesthesia (see above), a 10% solution of BDA in PBS was extensively injected into multiple loci along the central sulcus where regions representing not only the forelimb, but also the trunk and hindlimb were located, through a 5-μl Hamilton microsyringe (150 nl each penetration) (Fig. 1B).

Motoneuron labeling through the median nerve

To label spinal motoneurons through the median nerve on the SCI side, a 5% solution of WGA-HRP in physiological saline (Sigma-Aldrich) was applied to the cut end of the nerve four days prior to sacrifice. Under deep-anesthesia conditions (see above), the skin and intermuscular septum of the arm were dissected, and the median

nerve was exposed. The nerve was fully transected approximately 3.5 cm distal to the elbow joint. A total of 10 μl WGA-HRP was put inside a special tube, the cut end of the nerve was immersed in the tracer solution for 10 min, and then, the muscles and skin were sutured. Following the surgery, the monkeys were given the analgesic and antibiotic.

Histochemical and immunohistochemical procedures

Following sedation with ketamine hydrochloride (10 mg/kg, i.m.) and xylazine hydrochloride (1 mg/kg, i.m.), the monkeys were anesthetized deeply with sodium pentobarbital (50 mg/kg, i.v.) and perfused transcardially with 10% formalin. The fixed brain and spinal cord were removed, immersed in PBS containing 30% sucrose until they sank, and then cut serially into 40-μm thick transverse sections (for the spinal cord) or 50-μm thick frontal sections (for the brain) on a freezing microtome. Procedures for histochemical visualization of injected and transported BDA with DAB-nickel and for immunohistochemistry with the Vector NovaRed substrate kit (Vector laboratories) were done as described elsewhere (Nakagawa et al., 2015). For immunofluorescence histochemical procedures, floating sections were blocked with 2% normal goat or donkey serum and 3% bovine serum albumin in PBS containing 0.1% Triton X-100 for

60 min. The sections were then incubated with primary antibodies for 120 min at room temperature (RT), followed by two overnights at 4°C. Primary antibodies used in the present study were as follows: mouse anti-RGMa (IBL), rabbit anti-Iba1 (Wako), goat anti-ChAT (Millipore), mouse anti-NeuN (Millipore), goat anti-WGA (Vector laboratories), rabbit anti-WGA (Sigma-Aldrich), guinea pig anti-VGluT1 (Millipore), and sheep anti-Chx10 (Abcam) antibodies. The anti-WGA antibody was pre-absorbed with powder of the monkey's brain and spinal cord for prevention of cross-reaction with unknown endogenous molecules. The goat anti-WGA antibody was used for all analyses except double immunostaining with the rabbit anti-WGA antibody in combination with the goat anti-ChAT antibody. BDA immunofluorescence histochemistry was carried out with Alexa Fluor 488-conjugated streptavidin two overnights at 4°C. Subsequently, the sections were incubated with secondary antibodies for 120 min at RT in the dark. Secondary antibodies used in this study were as follows: goat and donkey anti-mouse, rabbit, goat, guinea pig, and sheep IgG Alexa Fluor 647, 568, and 488 (Invitrogen). To reduce endogenous autofluorescence, the sections were immersed in a TrueBlack (Biotium) solution diluted by 70% ethanol for 30 sec. All histochemical and immunohistochemical images were acquired with a microscope (Biorevo BZ-9000, Keyence) or a confocal laser-scanning microscope (Fluo View FV1000, Olympus and

298 LSM 800, Zeiss).

299

300 ***In situ* hybridization procedures**

301 Under deep anesthesia (see above), the monkeys underwent perfusion-fixation
302 with 4% paraformaldehyde (PFA) dissolved in 0.1 M phosphate buffer (PB; pH 7.4).
303 The brain was removed and immersed in a 30% sucrose solution containing 4% PFA at
304 4˚C overnight. *In situ* hybridization was performed as previously described with minor
305 modifications (Watakabe et al., 2007). Briefly, 40-μm-thick frontal sections were placed
306 onto glass slides (Thermo Fisher Scientific) and fixed with 4% PFA in PB for 15 min at
307 RT. The sections were treated sequentially with proteinase K (7.2 μg/ml) for 30 min at
308 37˚C, 4% PFA for 15 min at RT, 0.25% acetic anhydride in 0.1 M triethanolamine for 10
309 min at RT, 0.3% Triton X-100 in PB for 20 min at RT. Subsequently, the sections were
310 hybridized with a Digoxigenin (DIG)-labeled riboprobe (0.12 μg/ ml) for 16 hr at 68˚C
311 in a hybridization buffer comprising 50% formamide, 5x SSC, 5x Denhard's solution
312 (Invitrogen), 250 μg/ml tRNA (Roche Diagnostics), 500 μg/ml ssDNA (Sigma-Aldrich).
313 The riboprobe for *Neogenin* (XM_015142632.1; 346–979) was purchased from Geno
314 Staff (Tokyo, Japan) and heated at 80˚C for 5 min before use. After overnight, the
315 sections were washed with 0.2x SSC for 30 min x 3 at 68˚C. Next, the sections were

316 blocked with 1% blocking reagent (Roche Diagnostics) and 10% lamb serum in
317 Tris-buffered saline containing 0.05% Tween 20 (TBS) for 1 hr at RT and then
318 incubated with alkaline phosphatase-conjugated anti-DIG antibody (1:5,000 dilution,
319 Roche Diagnostics) in TBS containing 1% blocking reagent and 1% lamb serum for 2 hr
320 at RT. To visualize hybridization signals, the sections were immersed in a coloring
321 buffer containing nitroblue tetrazolium and 5-bromo-4-chloro-3-indolyl phosphate.
322
323 **Data analyses**
324 Quantification of BDA-labeled CST fibers below the lesioned site
325 BDA-labeled CST fibers in the C7, C8, and Th1 segments were quantified in
326 laminae VII and IX of transverse sections (400 μm apart) on the SCI side. Additionally,
327 BDA-labeled midline-crossing fibers from the ipsilateral and ventral CSTs were
328 quantified in each segment below the lesioned site. In lamina VII, the intensity of
329 BDA-labeled CST fibers stained by DAB reaction was measured within a rectangular
330 area (273 μm high x 362 μm wide) that was located 800 μm lateral to the center of the
331 central canal using an ImageJ software (National Institutes of Health, Bethesda, MD,
332 USA). Regarding lamina VII or IX, the number of contacts of BDA-labeled CST fibers
333 with single Chx10-labeled neuron (Immunofluorescence) or single WGA-HRP-labeled

334 motoneurons (DAB staining) was analyzed at a magnification of x400, respectively. The
335 contacts were defined by the presence of button-like swellings of BDA-labeled CST
336 fibers on somas or dendrites. The result was normalized by the mean number of
337 BDA-labeled CST fibers in the dorsolateral area at the C5 segment (three serial
338 sections) on the SCI side. BDA-labeled CST fibers that were observed in the gray
339 matter within a radius of 50 μm from the midline of the spinal cord on each of the SCI
340 and non-SCI sides were counted as midline-crossing fibers from the ipsilateral and
341 ventral CSTs (Fig. 5U). It should be noted here that such midline-crossing fibers may
342 contain some of contralaterally sprouting CST fibers. The result was normalized by the
343 mean number of BDA-labeled CST fibers in the dorsolateral area at each segment (three
344 serial sections) on the non-SCI side.
345
346 Measurements of the extent of spinal cord lesions
347 The extent of spinal cord lesions was measured, with the ImageJ software
348 described above, as the mean of the maximum lesioned area in three serial sections
349 which were Nissl-stained with 1% Cresyl violet (see also Nakagawa et al., 2015). The
350 lesioned area was expressed as the ratio to the total area of the hemi-transverse section
351 on the lesioned side.

352

353 **Statistics**

354 For behavioral analyses of the control antibody-treated and anti-RGMa
355 antibody-treated monkey groups, two-way ANOVA was applied. Increases in
356 BDA-labeled CST fibers in laminae VII, IX and the midline area (i.e., midline-crossing
357 CST fibers) were analyzed by two-way ANOVA, followed by Student's *t*-test. For
358 within-group comparisons for pre- versus post-muscimol injections in the
359 reaching/grasping task and for the extent of spinal lesions, paired *t*-test was applied. All
360 data were represented as mean ± S.E.M., and statistical significance was accepted at $P <$
361 0.05.

362

Results

SCI model and the extent of spinal cord lesions

In our SCI model, the spinal cord was unilaterally lesioned in macaque monkeys. The lesions were made at the border between the C6 and the C7 level to infringe upon the lateral area of the hemi-transverse section (Fig. 1A). When BDA was injected into the contralateral (contralesional) MI, laterally-situated CST fibers were found to be fully removed in all of the lesioned monkeys, and, therefore, no BDA-labeled CST fibers in any cases were observed in the dorsolateral funiculus of the spinal cord below the lesioned site (Figs. 1B-E,G-I and 2A; see also Fig. 5B,G,L). The lesioned sites in all SCI monkeys were Nissl-stained to assess the ratio of the lesioned area, and there was no marked difference between the control antibody-treated (control) monkey group and the anti-RGMa antibody-treated (RGMa antibody-treated) monkey group (Fig. 2A,B). Part of the medial gray matter was kept intact to retain a route of sprouting CST fibers in our SCI model, and anterograde tract-tracing with BDA from the contralesional MI resulted in CST fiber labeling in this area (Figs. 1C,D,F,H,J and 2A). To confirm cross-reaction of the anti-RGMa antibody to the MI and the spinal cord of rhesus monkeys, western blotting was performed. We observed double and triple bands in the monkey MI and spinal cord (Fig. 1M). It has been reported that the RGMa protein is a tethered

membrane-bound molecule, and that proteolytic processing amplifies RGMa diversity by creating soluble versions, the full-length and proteolytic cleavage RGMa, with long-range effects (Tassew et al., 2009, 2012). The antibody was delivered continuously to the lesioned site via the osmotic pump for four weeks immediately after SCI (Fig. 1K,L,N).

Upregulation of RGMa around the lesioned site after SCI

First, the expression patterns of RGMa and *Neogenin* (a receptor for RGMs) were examined by immunohistochemistry or *in situ* hybridization in the cervical cord or MI, respectively, in our SCI model (one intact and two lesioned monkeys; Fig. 3). Longitudinal sections in the cervical cord ten days after SCI were immunostained with the anti-RGMa antibody, and then the RGMa expression was compared with a region remote from the lesioned site in the same section and with the same region in an intact (uninjured) section (Fig. 3A–C,F). Our immnunohistochemical analyses revealed that the RGMa expression was obviously increased around the lesioned site after SCI. Next, we characterized RGMa-expressing cells by double immunofluorescence histochemistry and found that RGMa was present in Iba1-positive cells (Fig. 3D–F). Thus, RGMa was expressed in microglia/macrophages and upregulated specifically around the lesioned

399 site. In addition, *Neogenin* was expressed in layer 5 (identified in the adjacent
400 Nissl-stained sections) of the contralesional and ipsilesional MI (Fig. 3G–J).
401
402 **Effects of anti-RGMa antibody on impaired manual dexterity after SCI**
403 In the reaching/grasping task, the motor performance through both the
404 vertical-slot and the horizontal-slot tasks was greatly recovered in the RGMa
405 antibody-treated monkey group, compared with the control monkey group, to reach as
406 highly as the pre-SCI level (Fig. 4C,D, Video S1). Similar results were obtained in the
407 modified Brinkman board test, especially when the RGMa antibody-treated monkey
408 group took out pellets from vertical slots (Fig. 4F,G, Video S2). In the case where skilled
409 forelimb movements through the horizontal-slot task were attempted, the RGMa
410 antibody-treated monkey group did not so prominently exhibit functional recovery,
411 although motor behavior was improved in comparison with the control monkey group in
412 which no such movements were restored at all (Fig. 4H, Video S2). Moreover, our
413 behavioral analyses revealed that in both the reaching/grasping task and the modified
414 Brinkman board test, the antibody treatment against RGMa not only promoted the
415 recovery of motor functions, but also advanced the start of recovery following SCI (Fig.
416 4C,D,F–H).

Increase in sprouting CST fibers with the neutralizing antibody against RGMa

To begin with addressing the reorganization of CST fibers below the lesioned site, we analyzed the distribution pattern of BDA-labeled CST fibers in the C7, C8, and Th1 segments. We observed no BDA-labeled CST fibers in the dorsolateral funiculus in both the control and the RGMa antibody-treated monkey groups (Fig. 5A,B,F,G,K,L). Approximately 30–50% of the BDA-labeled CST fibers, relative to an intact monkey, was found in lamina VII of the RGMa antibody-treated monkey group, whereas less than 10% of them were seen in lamina VII of the control monkey group (Fig. 5A,C,F,H,K,M,P). In lamina IX, all WGA-HRP-labeled neurons corresponded with ChAT-positive motoneurons (Fig. 5D'), indicating that all of them are motoneurons for the median nerve. In the RGMa antibody-treated monkey group, the number of contacts of sprouting CST fibers with single WGA-positive neurons was increased in lamina IX below the lesioned site, compared with the control monkey group (Fig. 5A,D,E,F,I,J,K,N,O,Q,E'). At least part of the sprouting CST fibers seemed to be in contact with spinal interneurons immunolabeled for Chx10. Similarly, we observed that the sprouting CST fibers in the RGMa antibody-treated monkey group appeared to make contact with single Chx10-positive neurons more frequently than in the control monkey

group (Fig. 5W-B',C'). We found a certain difference in the reinnervation pattern of sprouting CST fibers in each segment. In lamina VII, the intensity of BDA-labeled CST fibers and the number of contacts of these CST fibers with single Chx10-positive neurons were gradually decreased as the distance from the lesioned site became larger (C7 < C8 < Th1) in the RGMa antibody-treated monkey group. By contrast, the number of contacts of sprouting CST fibers with single WGA-positive neurons was increased in the same group, which was similar to the findings in an intact monkey (Fig. 5P,Q,C'). The number of midline-crossing fibers was also increased by the neutralizing antibody against RGMa (Fig. 5R–V). It should be noted here that the midline-crossing fibers observed may involve some extended fibers from the injured CST.

Impairments in recovered manual dexterity by muscimol inactivation in the contralesional MI

Following all behavioral analyses, ICMS was performed in the contralesional and ipsilesional MI of both the control and the RGMa antibody-treated monkey groups whether the contralesional MI might contribute to the functional recovery from impaired manual dexterity due to SCI (Fig. 1N). The movements of the digits ipsilateral to SCI were successfully elicited by intracortical microstimulation in four loci of the

453 contralesional MI, but not of the ipsilesional MI in the RGMa antibody-treated SCI
454 monkeys (Fig. 6A). Subsequent injections of muscimol into all of the
455 electrophysiologically-identified digit region of the contralesional MI, but not of the
456 ipsilesional MI, induced reversible impairments in skilled forelimb movements on the
457 SCI side (Fig. 6C,D). The reaching/grasping task (for horizontal slots) was employed to
458 assess the motor function. About 20 min after the muscimol injections, manual dexterity
459 was gradually deteriorated and severely impaired within one hour. Thereafter, impaired
460 forelimb movements were continually seen for a few hours. Although all RGMa
461 antibody-treated monkeys could move the digits individually on the next day, manual
462 dexterity was not so sufficiently restored, as compared to that before the muscimol
463 injections into the contralesional MI. When we carried out the ICMS experiment in the
464 control monkey group, no movements of the digits were evoked in the contralesional MI
465 (Fig. 6B). In general, the digit region of the MI was surrounded by the regions
466 representing the wrist, elbow, and face in macaque monkeys (Sessle and Wiesendanger,
467 1982). However, a sector surrounded by the wrist, elbow, and face regions exhibited no
468 response to ICMS (Fig. 6B). As we could not identify the digit region in the
469 contralesional MI of the control monkey group, we injected muscimol only into the
470 ipsilesional MI. Then, the muscimol injections into the digit region of the ipsilesional MI

471 induced reversible impairments in skilled movements of the SCI-unimpaired forelimb
472 only on the uninjured side (Fig. 6E), just like the RGMa antibody-treated monkey group
473 (Fig. 6D).
474

Discussion

Owing to the low capacity of growth/regeneration in the mature CNS, various therapeutic approaches to CNS injures have been attempted against extrinsic and intrinsic inhibiting factors using *in vivo* and *in vitro* experiments with rodents (Sandvig et al., 2004; Hata et al., 2006; Mar et al., 2014). According to previous works (Yiu and He, 2006; Popovich and Longbrake, 2008; Rolls et al., 2009) glial cells expressing growth-inhibiting factors are rich in the lesioned area after SCI in rodents, and immune and inflammatory cells are also accumulated in the same area. It has repeatedly been demonstrated that RGMa is expressed in these cells (Schwab et al., 2005; Mirakaj et al., 2010; Muramatsu et al., 2011). The present study revealed that RGMa was specifically upregulated around the lesioned site with increases in microglia/macrophages after SCI (see Fig. 3D,E).

The spinal cord repair strategies through growing/regenerating axons include a series of events, consisting of the initiation of axonal growth, the maintenance of axonal elongation, the connectivity with appropriate target neurons, and the reorganization of neural circuitry (Bradbury and McMahon, 2006). In rodent SCI models, a reaching/grasping behavior was promoted by enhanced sprouting CST fibers, and many of these fibers were extended through the medial part of the spinal cord (Hollis et al.,

493 2016). Thus, the enhanced sprouting CST fibers would make a synaptic connection with
494 spinal interneurons as the target for restoration of forelimb functions in rodents. For a
495 precision grip in higher primates, corticomotoneuronal pathway neurons in the MI are
496 specifically activated (Muir and Lemon, 1983). Moreover, during the monkey's
497 performance of a pinching task, motor commands descending to spinal motoneurons are
498 mediated at least partly by the spinal interneurons (Takei and Seki, 2010, 2013). Taken
499 together, it is most likely that the reorganization of both the direct and the indirect (via
500 the spinal interneurons) corticomotoneuronal pathways is required to promote recovery
501 from impaired manual dexterity through enhanced sprouting of CST fibers in our SCI
502 model.

503 In our behavioral tasks, to take out pellets skillfully from vertical and horizontal
504 slots, cortically-derived compensatory input would be transmitted to the motoneurons
505 and/or interneurons in the C7, C8, and Th1 segments that are situated below the SCI site.
506 Particularly when taking out a pellet from the horizontal slot in the modified Brinkman
507 board test, the monkey is required to move the wrist to the ulnar direction for achieving
508 digit flexion with ulnar deviation. It has been reported that the wrist angle in the ulnar
509 direction is largely reduced after SCI when the monkey takes out a pellet from the
510 horizontal slot (Hoogewoud et al., 2013). In macaque monkeys, spinal motoneurons

innervating the extensor carpi ulnaris muscle responsible for digit flexion with ulnar deviation are mainly distributed in the C8 and Th1 segments (Jenny and Inukai, 1983; Schieber, 1995).

We demonstrated that sprouting CST fibers originating from the contralesional MI in RGMa antibody-treated monkeys penetrated more densely, compared with the control monkey group, into laminae VII and IX where spinal interneurons and motoneurons were located, respectively, below the lesioned site (see Fig. 5P,Q). In our experiments, the motoneurons in the C7, C8, and Th1 segments were labeled through the median nerve that predominantly governs the distal forelimb muscles, activity of which is essential for execution of manual dexterity with a precision grip (Dun et al., 2007). In addition, a large number of motoneurons for hand (digits) muscles in primates are located in the Th1 segment (Jenny and Inukai, 1983). With respect to the pattern of reinnervation of the enhanced corticomotoneuronal pathway after SCI with the anti-RGMa antibody treatment, sprouting CST fibers might lead to appropriate target motoneurons with guidance factors to promote the recovery of motor functions effectively and efficiently.

At least part of sprouting CST fibers seemed to be in contact with the interneurons immunolabeled for Chx10. Chx10 was originally identified as one of the

markers for glutamatergic interneurons in rodents (Ericson et al., 1997), and Chx10-positive neurons are reportedly distributed throughout the hindbrain and the spinal cord in mammals and regulate motor functions, such as breathing and locomotion (Ai-Mosawie et al., 2007; Crone et al., 2008, 2012; Dougherty and Kiehn, 2010; Azim et al., 2014). According to a recent work (Liu et al., 2015), there is a correlation between the number of Chx10-positive neurons in contact with sprouting CST fibers and functional recovery of the forelimb with unilateral cervical cord injury in mice. Together with the direct corticomotoneuronal pathway, the compensatory indirect pathway via spinal interneurons may also be crucial to the recovery of a series of forelimb movements, reaching for slots and taking out pellets from slots using a precision grip, in our SCI model.

Interestingly, according to our behavioral analyses, the antibody treatment against RGMa not only promoted the recovery of motor functions, i.e., the ability to move the digits individually, but also advanced the start of recovery following SCI. It has been well documented that treatment with the RGMa-neutralizing antibody in a rodent model of multiple sclerosis promotes functional recovery by preventing neurodegeneration (Muramatsu et al., 2011; Tanabe and Yamashita, 2014; Demicheva et al., 2015). Recently, it has been reported that the RGMa antibody treatment promoted

547 neuronal survival around the lesioned site with improvement of functional recovery in a
548 rodent SCI model (Mothe et al., 2017). Moreover, RGMa has been shown to reduce
549 leukocyte trafficking and retard inflammation (Mirakaj et al., 2010). Thus, RGMa
550 suppression has a certain impact on neuroprotection as well as on neurite outgrowth,
551 and, therefore, the present results might be ascribed, at least partly, to the
552 neuroprotective effect of the RGMa antibody.

553 The spinal cord lesions in some cases (i.e., Ctrl-B and RGMa-A monkeys)
554 infringed, to some extent, upon uncrossed ventral CST region, though it almost
555 unaffected recovery of manual dexterity, especially in the RGMa antibody-treated
556 (RGMa-A) monkey (data not shown). It has previously been reported that the ventral
557 CST distributes the fibers to proximal muscles, such as the neck, trunk, and proximal
558 upper extremities (Nyberg-Hansen, 1963; Davidoff, 1990; Canedo, 1997). The motor
559 tasks that we used in the present work (i.e., reaching/grasping task and the modified
560 Brinkman board test) are required for movements of the proximal upper limb, but the
561 spinal region responsible for the proximal upper limb remains intact in our SCI model.

562 By carrying out a series of pharmacological experiments following ICMS, we
563 have demonstrated that the contralesional MI is greatly involved in recovery from
564 impaired manual dexterity in our SCI model with the anti-RGMa antibody treatment. In

565 the control monkey group, on the other hand, forelimb movements once impaired by
566 SCI could not be evoked at all by our ICMS protocol (44-pulse train, 65-μA current).
567 This may depend on an increase in sprouting CST fibers from the contralesional MI to
568 the cervical cord on the injured side. Additionally, it should be noted here that other
569 descending pathways, including the cortico-brainstem and cortico-propriospinal
570 pathways, might contribute to the functional recovery (Isa et al., 2013). In a similar
571 primate model of SCI (C7/C8 lesion model), reorganization of CST fibers originating
572 from the contralesional MI with the somatotopic map altered is crucial to recovery of
573 motor functions (Schmidlin et al., 2004, 2005). Part of uncrossed CST fibers derived
574 from the ipsilesional MI was disrupted in our SCI model, and, also, *Neogenin* was
575 expressed in layer 5 of the ipsilesional MI as well as of the contralesional MI (see Fig.
576 3I,J). RGMa has been shown to evoke the strong inhibition of axonal outgrowth and
577 regrowth through the transmembrane receptor, Neogenin (Tassew et al., 2014). Hence, it
578 can be considered that injured CST fibers extend beyond the lesioned site from the
579 ipsilesional MI by the aid of the anti-RGMa antibody. However, the CST fibers arising
580 from the ipsilesional MI may not work as a functional wiring at a late stage after SCI. In
581 view of the fact that the ipsilesional MI is activated at an early, but not a late stage of
582 recovery in a different primate model of SCI (Nishimura et al., 2007), the ipsilesional

583 MI might participate in functional restoration only transiently.

584 The present study defines that RGMa is a critical target molecule to promote
585 recovery from impaired manual dexterity after SCI. The antibody treatment against
586 RGMa may probably be applied not only to SCI, but also to other CNS insults, such as
587 traumatic brain injuries, stroke, and multiple sclerosis.

588

Funding

This work was supported by Core Research for Evolutional Science and Technology (CREST) from Japan Science and Technology Agency, Strategic Research Program for Brain Sciences from Japan Agency for Medical Research and Development, and Grants-in-Aid for Scientific Research on Innovative Areas (to M.T., 15H01434) and for Young Scientists (B) (to H.N.) from the Ministry of Education, Culture, Sports, Science, and Technology of Japan.

Notes

We thank K. Koide, R. Yasukochi, Y. Takata, and H. Yamanaka for technical assistance. The authors declare no competing financial interests.

601 **References**

602 AI-Mosawie A, Wilson JM, Brownstone RM. 2007. Heterogeneity of V2-derived
603 interneurons in the adult mouse spinal cord. Eur J Neurosci. 26:3003–3015.

604 Azim E, Jiang J, Alstermark, B, Jessell TM. 2014. Skilled reaching relies a V2a
605 propriospinal internal copy circuit. Nature. 508:357–363.

606 Bradbury EJ, McMahon SB. 2006. Spinal cord repair strategies: why do they work? Nat
607 Rev Neurosci. 7:644–653.

608 Canedo A. 1997. Primary motor cortex influences on the descending and ascending
609 systems. Prog Neurobiol. 51:287–335.

610 Crone SA, Quinlan KA, Zagoraiou L, Droho S, Restrepo CE, Lundfald L, Endo T,
611 Setlak J, Jessell TM, Kiehn O, et al. 2008. Genetic ablation of V2a ipsilateral
612 interneurons disrupts left-right locomotor coordination in mammalian spinal cord.
613 Neuron. 60:70–83.

614 Crone SA, Viemari JC, Droho S, Mrejeru A, Ramirez JM, Sharma K. 2012. Irregular
615 breathing in mice following geneticablation of V2a neurons. J Neurosci.
616 32:7895–7906.

617 Davidoff RA. 1990. The pyramidal tract. Neurology. 40:332-339.

618 Demicheva E., Cui YF, Bardwell P, Barghom S, Kron M, Meyer AH, Schmidt M,
619 Gerlach B, Leddy M, Barlow E, et al. 2015. Targeting repulsive guidance molecule
620 A to promote regeneration and neuroprotection in multiple sclerosis. Cell Rep.
621 10:1887–1898.
622 Dougherty KJ, Kiehn O. 2010. Functional organization of V2a-related locomotor
623 circuits in the rodent spinal cord. Ann. NY Acad Sci. 1198:85–93.
624 Dun S, Kaufmann RA, Li ZM. 2007. Lower median nerve block impairs precision grip.
625 J Electromyogr Kinesiol. 17:348–354.
626 Ericson J, Rashbass P, Schedl A, Brenner-Morton S, Kawakami A, van Heyningen V,
627 Jessell TM, Briscoe J. 1997. Pax6 controls progenitor cell identify and neuronal
628 fate in response to graded Shh signaling. Cell. 90:1169–180.
629 Freund P, Schmidlin E, Wannier T, Bloch J, Mir A, Schwab ME, Rouiller, EN. 2006.
630 Nogo-A–antibody treatment enhances sprouting and functional recovery after
631 cervical lesion in adult primates. Nat Med. 12:790–792.
632 Freund P, Schmidlin E, Wannier T, Bloch J, Mir A, Schwab ME, Rouiller EN. 2009.
633 Anti-Nogo–A antibody treatment promotes recovery of manual dexterity after
634 unilateral cervical lesion in adult primates – re-examination and extension of
635 behavioral data. Eur J Neurosci. 29:983–996.

636 GrandPré T, Li S, Strittmatter SM. 2002. Nogo-66 receptor antagonist peptide promotes
637 axonal regeneration. Nature. 417:547–551.
638 Hata K, Fujitani M, Yasuda Y, Doya H, Saito T, Yamagishi S, Mueller BK, Yamashita
639 T. 2006. RGMa inhibition promotes axonal growth and recovery after spinal cord
640 injury. J Cell Biol. 173:47–58.
641 Hollis ER 2nd, Ishiko N, Yu T, Lu CC, Haimovich A, Tolentino K, Richman A, Tury A,
642 Wang SH, Pessian M, et al. 2016. Ryk controls remapping of motor cortex during
643 fanctional recovery after spinal cord injury. Nat Neurosci. 19:697–705.
644 Hoogewoud F, Hamadjida A. Wyss AF, Mir A, Schwab ME, Belhaj-Saif A, Rouiller
645 EM. 2013. Comparison of functional recovery of manual dexterity after unilateral
646 spinal cord lesion or motor cortex lesion in adult macaque monkeys. Front Neurol.
647 4:101.
648 Isa T, Kinoshita M, Nishimura Y. 2013. Role of direct vs. indirect pathways from the
649 motor cortex to spinal motoneurons in the control of hand dexterity. Front Neurol.
650 4:191.
651 Jenny AB, Inukai J. 1983. Principles of motor organization of the monkey cervical
652 spinal cord. J Neurosci. 3:567–575.

Lah GL, Key B. 2012. Dual roles of the chemorepellent axon guidance molecule RGMa in establishing pioneering axon tracts and neural fate decisions in embryonic vertebrate forebrain. Dev Neurobiol. 72:1458–1470.

Lemon RN. 1993. The G. L. Brown Prize Lecture. Cortical control of the primate hand. Exp Physiol. 78:263–301.

Liu ZH, Yip PK, Adams L, Davies M, Lee JW, Michael GJ, Priestley JV, Michael-Titus AT. 2015. A single bolus of docosahexaenoic acid promotes neuroplastic changes in the innervation of spinal cord interneurons and motor neurons and improves functional recovery after spinal cord injury. J Neurosci. 35:12733–12752.

Mar FM, Bonni A, Sousa MM. 2014. Cell intrinsic control of axon regeneration. EMBO Rep. 15:254–263.

Matsunaga E, Nakamura H, Chedotal A. 2006. Repulusive guidance molecule plays multipleroles in neuronal differentiation and axon guidance. J Neurosci. 26:6082–6088.

Matsunaga E, Tauszing-Delamasure S, Monnier PP, Mueller BK, Strittmatter SM, Mehlen PCHedotal A. 2004. RGM and its receptor neogenin regulate neuronal survival. Nat Cell Biol. 6:749–755.

Mirakaj V, Brown S, Laucher S, Steinl C, Klein G, Köhler D, Skutella T, Meisel C, Brommer B, Rosenberger P, et al. 2010. Repulsive guidance molecule-A (RGM-A) inhibits leukocyte migration and mitigates inflammation. Proc Natl Acad Sci USA. 108:6555–6560.

Miyachi S, Lu X, Inoue S, Iwasaki T, Koike S, Nambu A, Takada M. 2005. Organization of multisynaptic inputs from prefrontal cortex to primary motor cortex as revealed by retrograde transneuronal transport of rabies virus. J Neurosci. 25:2547–2556.

Monnier PP, Sierra A, Macchi P, Deitinghoff L, Andersen JS, Mann M, Flad M, Homberger MR, Stahl B, Bonhoeffer F, Mueller BK. 2002. RGM is a repulsive guidance molecule for retinal axons. Nature. 419:392–395.

Mothe AJ, Tassew NG, Shabanzadeh AP, Penheiro R, Vigouroux RJ, Huang L, Grinnell C, Cui YF, Fung E, Monnier PP, et al. 2017. RGMa inhibition with human monoclonal antibodies promotes regeneration, plasticity and repair, and attenuates neuropathic pain after spinal cord injury. Sci Rep. 7:10529.

Muir RB, Lemon RN. 1983. Corticospinal neurons with a special role in precision grip. Brain Res. 261:312–316.

687 Muramatsu R, Kubo T, Mori M, Nakamura Y, Fujita Y, Akutsu T, Okuno T, Taniguchi
688 J, Kumanogoh A, Yoshida M, et al. 2011. RGMa modulates T cell responses and is
689 involved in autoimmune encephalomyelitis. Nat Med. 17:488–494.
690 Nakagawa H, Ninomiya T, Yamashita T, Takada M. 2015. Reorganization of
691 corticospinal tract after spinal cord injury in adult macaques. Sci Rep. 5:11986.
692 Nishimura Y, Onoe H, Morichika Y, Perfiliev S, Tsukada H, Isa T. 2007.
693 Time-dependent central compensatory mechanisms of finger dexterity after spinal
694 cord injury. Science. 318:1150–1155.
695 Nyberg-Hansen R. 1963. Some comments on the pyramidal tract, with special reference
696 to its individual variations in man. Acta Neurol Scand. 39:1–30.
697 Oudega M, Perez MA. 2012. Corticospinal reorganization after spinal cord injury. J
698 Physiol. 590:3647–3663.
699 Popovich PG, Longbrake EE. 2008. Can the immune system be harnessed to repair the
700 CNS? Nat Rev Neurosci. 9:481–493.
701 Rolls A, Shechter R, Schwartz M. 2009. The bright side of the glial scar in CNS repair.
702 Nat Rev Neurosci. 10:235–241.

703 Rouiller EM, Yu XH, Moret V, Tempini A, Wiesendanger M, Liang E, 1998. Dexterity
704 in adult monkeys following early lesion of the motor cortical hand area: the role of
705 cortex adjacent to the lesion. Eur J Neurosci. 10:729–740.
706 Sandvig A, Berry M, Butt A, Longan A. 2004. Myelin-, reactive glia-, and scar-derived
707 CNS axon growth inhibitors: expression, receptor signaling, and correlation with
708 axon regeneration. Glia. 46:225–251.
709 Schieber MH. 1995. Muscular production of individuated finger movements: the roles
710 of extrinsic finger muscles. J Neurosci. 15:284–297.
711 Schmidlin E, Wannier T, Bioch J, Ruiller EM. 2004. Progressive plastic change in the
712 hand representation of the primary motor cortex parallel incomplete recovery from
713 a unilateral section of the corticospinal tract at cervical level in monkeys. Brain Res.
714 1017:172–183.
715 Schmidlin E, Wannier T, Bioch J, Belhaj-Saif A, Wyss AF, Ruiller EM. 2005.
716 Reduction of the hand representation in the ipsilateral primary motor cortex
717 following unilateral section on the corticospinal tract at cervical level in monkeys.
718 BMC Neurosci. 6:56.

719 Schwab JM, Conrad S, Monnier PP, Julien S. Mueller BK, Schluesener HJ. 2005.
720 Spinal cord injury-induced lesional expression of the repulsive guidance molecule
721 (RGM). Eur J Neurosci. 21:1569–1576.
722 Sessle BJ, Wiesendanger M. 1982. Structural and functional definition of the motor
723 cortex in the monkey (*Macaca fascicularis*). J Physiol. 323:245–265.
724 Stahl B, Muller B, von Boxberg Y, Cox, EC, Bonhoeffer F. 1990. Biochemical
725 characterization of a putative axonal guidance molecule of the chick visual system.
726 Neuron. 5:735–743.
727 Takei T, Seki K. 2010. Spinal interneurons facilitate coactivation of hand muscles
728 during a precision grip task in monkeys. J Neurosci. 30:17041–17050.
729 Takei T, Seki K. 2013. Spinal premotor interneurons mediate dynamic and static motor
730 commands for precision grip in monkeys. J Neurosci. 33:8850–8860.
731 Tanabe S, Yamashita T. 2014. Repulusive guidance molecule-a is involved in
732 Th17-cell-induced neurodegeneration in autoimmune encephalomyelitis. Cell Rep.
733 9:1459–1470.
734 Tassew NG, Charish J, Chestopalova L, Monnier PP. 2009. Sustained *in vivo* inhibition
735 of protein domains using single-chain Fv recombinant antibodies and its application
736 to dissect RGMa activity on axonal outgrowth. J Neurosci. 29:1126–1131.

737 Tassew NG, Charish J, Seidah NG, Monnier PP. 2012. SKI-1 and Furin generate
738 multiple RGMa fragments that regulate axonal growth. Dev Cell. 22:391‑402.
739 Tassew NG, Mothe AJ, Shabanzadeh AP, Banerjee P, Koeberle PD, Bremner R, Tator
740 CH, Monnier PP. 2014. Modifying lipid rafts promotes regeneration and functional
741 recovery. Cell Rep. 8:11146–1159.
742 Vavrek R, Girgis J, Tetzlaff W, Hiebert GW, Fouad K. 2006. BDNF promotes
743 connections of corticospinal neurons onto spared descending interneurons in spinal
744 cord injured rat. Brain. 129:1534–1545.
745 Wahl AS, Omlor W, Rubio JC, Chen JL, Zheng H, Schröter A, Gullo M, Weinmann O,
746 Kobayashi K, Helmchen F, et al. 2014. Neuronal repair. Asynchronous therapy
747 restores motor control by rewiring of the rat corticospinal tract after stroke. Science.
748 34:1250–1255.
749 Watakabe A, Ichinohe N, Ohsawa S, Hashikawa T. Komatsu Y, Rockland KS,
750 Yamamori T. 2007. Comparative analysis of layer-specific genes in Mammalian
751 neocortex. Cereb Cortex. 17:1918–1933.
752 Yiu G, He Z. 2006. Glial inhibition of CNS axon regeneration. Nat Rev Neurosci.
753 7:617–627.
754

Figure legends

Figure 1. SCI model and experimental time-course.

(A) Schematic diagram showing our primate model of SCI. Unilateral lesions were made at a border between the C6 and the C7 segment. Asterisk indicates the lesioned site. (B) Example of the injection site in the contralesional MI. (C and G) Nissl-stained transverse sections in the injured (SCI) and uninjured spinal cords. The strongly stained area represents the lesion extent in panel C. (D and H) Transverse sections labeled with BDA injected into the contralesional or contralateral MI in the injured or uninjured spinal cord, respectively. The dotted line demarcates the lesioned area in panel D. (E and I) Higher-power magnifications of areas in the dorsolateral funiculus in panels D and H, respectively. (F and J) Higher-power magnifications of areas in the medial gray matter in panels D and H, respectively. Note that BDA-labeled CST fibers extend beyond the lesioned site through the intact medial gray matter in the injured spinal cord. (K) Schematic diagram showing the antibody delivery system using an osmotic pump. (L) Anti-RGMa antibody delivered around the lesioned site via an osmotic pump. To visualize the extent of antibody infusion, Fast blue was used. (M) Western blot analysis of the anti-RGMa antibody. The antibody crosses to the MI and the spinal cord of a rhesus

772 monkey. (N) Experimental time-course. Scale bars, B and C 1 mm for B to D and G, H,
773 for B, C, E; J 50 μm for E, F, I and J.

774

775 **Figure 2. Extent of spinal cord lesions.**

776 (A) Extent of SCI (in blue) in a representative transverse section in each monkey. (B)
777 Ratio of the lesioned area to the total area in a hemisection in each of control
778 antibody-treated (Ctrl) and anti-RGMa antibody-treated (RGMa) monkeys. There is no
779 marked difference in the averaged ratio between the two monkey groups. Because of the
780 death by unknown accident shortly after the behavioral analyses, monkey RGMa-B was
781 excluded from the electrophysiological/pharmacological and histological analyses.

782

783 **Figure 3. Expression patterns of RGMa and *Neogenin* in the cervical cord and MI.**

784 (A) RGMa expression (in purple) around the lesioned site (at the C6/C7 border) 10 days
785 after SCI in a longitudinal section. Shown in black are CST fibers anterogradely labeled
786 after BDA injections into the contralesional MI. (B) RGMa expression in a region
787 remote from the lesioned site in the same section. (C) RGMa expression in the same
788 region as in panel A in a normal (uninjured) case. (D and E) Expression of RGMa in
789 combination with Iba1 around the lesioned site. (F) Schematic diagram representing the

approximate locations of panels A, B, D, and E. (G) *In situ* hybridization for *Neogenin* messenger RNA in layer 5 (V) of the contralesional MI 10 days after SCI in a frontal section. (H) Higher-power magnification of a square area in panel G. (I) *In situ* hybridization for *Neogenin* messenger RNA in layer 5 (V) of the ipsilesional MI 10 days after SCI in a frontal section. (J) Higher-power magnification of a square area in panel I. Scale bars, A, 50 μm for A to C; D,G,I, 200 μm; E,H,J, 50 μm.

Figure 4. Recovery from impaired manual dexterity with the neutralizing antibody against RGMa.

(A and B) Reaching/grasping task. The monkey reaches for vertical (A) or horizontal (B) slots and grasps pellets. (C and D) Ratio of pellets collected through vertical (C) or horizontal (D) slots. (E) Modified Brinkman board test. The monkey takes out pellets from randomly-set vertical and horizontal slots. (F) Total number of pellets collected through vertical and horizontal slots. (G and H) Number of pellets collected through vertical (G) or horizontal (H) slots. All data are based on three control antibody-treated (Ctrl) and four anti-RGMa antibody-treated (RGMa) monkeys. Error bars denote S.E.M. (two-way ANOVA, $*P < 0.05$).

Figure 5. Sprouting of CST fibers with the neutralizing antibody against RGMa.

(A, F, and K) BDA-labeled CST fibers in the Th1 segment in an intact (Uninjured; A), a control antibody-treated (Ctrl; F) and an anti-RGMa antibody-treated (RGMa; K) monkey. (B, G, and L) Higher-power magnifications of areas of the dorsolateral funiculus in panels A, F, and K, respectively. (C, H, M, D, I, and N) Higher-power magnifications of areas of laminae VII (C, H, and M) and IX (D, I, and N) in panels A, F, and K, respectively. (E, J, and O) Higher-power magnifications of dotted zones in panels D, I, and N, respectively. (P) Intensity of BDA-labeled CST fibers in lamina VII in the intact (Uninjured; n = 1), control antibody-treated (Ctrl; n = 3), and anti-RGMa antibody-treated (RGMa; n = 3) monkey groups. (Q) Number of contacts of BDA-labeled CST fibers with single WGA-positive motoneurons in lamina IX in the same monkey groups as in panel P. (R, S, and T) BDA-labeled CST fibers crossing the midline of the spinal cord in an intact (Uninjured; R), a control antibody-treated (Ctrl; S), and an anti-RGMa antibody-treated (RGMa; T) monkey. BDA was injected into the contralateral or contralesional MI. (U) Schematic diagram showing the midline area examined. CC, central canal. (V) Number of midline-crossing CST fibers below the lesioned site (i.e., C7, C8, and Th1 segments). (W, Y, and A') Spinal interneurons triple-labeled for BDA, NeuN, and Chx10 in lamina VII of the Th1 segment in an intact

826 (Uninjured; W), a control antibody-treated (Ctrl; Y), and an anti-RGMa antibody-treated
827 (RGMa; A') monkey. (X, Z, and B') Higher-power magnifications of dotted zones in
828 panels W, Y, and A', respectively. BDA-labeled CST fibers in contact with single
829 Chx10-positive neurons (specified by arrowheads). (C') Number of contacts of
830 BDA-labeled CST fibers with single Chx10-positive neurons in lamina VII in the same
831 monkey groups as in panels P and Q. (D') Motoneurons double-labeled for WGA-HRP
832 through the median nerve and ChAT in lamina IX of the Th1 segment in an anti-RGMa
833 antibody-treated monkey. All WGA-HRP-labeled neurons are ChAT-positive. The
834 dotted line indicates the border between the gray and the white matter. (E') Triple
835 labeling for BDA, WGA-HRP, and VGluT1 in lamina IX of the Th1 segment in an
836 anti-RGMa antibody-treated monkey. A BDA-labeled CST fiber in contact with a single
837 WGA-positive motoneuron (specified by arrowheads). Scale bars, A, 1 mm for A,F,K; N,
838 100 μm for B to D, G to I, L to N; O, 50 μm for E, J and O; R, 100 μm for R, S and T; W,
839 200 μm for W, Y and A'; X and D', 5 μm for X, Z, B' and D'; C', 200 μm. Error bars
840 denote S.E.M. (two-way ANOVA, followed by Student's *t*-test, $*P < 0.05$).
841
842 **Figure 6. Effects of muscimol injections into the MI on manual dexterity.**

(A) Sites of muscimol injections into the contralesional and ipsilesional MI in a representative anti-RGMa antibody-treated monkey (RGMa-A). Filled circles indicate the injection loci in all of which ICMS induced movements of the digits on the contralateral side. AS, arcuate sulcus; CS, central sulcus. Scale bar, 2 mm. (B) Results of ICMS mapping of the contralesional MI in a representative control antibody-treated monkey (Ctrl-C). Each letter denotes the electrophysiologically-identified body part as follows: E, elbow; F, face; W, wrist; X, no response. Scale bar, 2 mm. (C–E) Skilled movements after muscimol injections into the digit region of the contralesional MI (C) or the ipsilesional MI (D) in the anti-RGMa antibody-treated monkey group ($n = 3$), or of the contralesional MI in the control antibody-treated monkey group (E; $n = 3$). Manual dexterity that had been impaired by SCI and then recovered by RGMa treatment (SCI-impaired forelimb) was again impaired after muscimol (but not saline) injections into the contralesional MI. On the other hand, the muscimol injections into the ipsilesional MI only caused impairments in skilled movements of the normal forelimb (SCI-unimpaired forelimb) contralateral to the injections. Error bars indicate S.E.M. (Student's *t*-test, $*P < 0.05$).

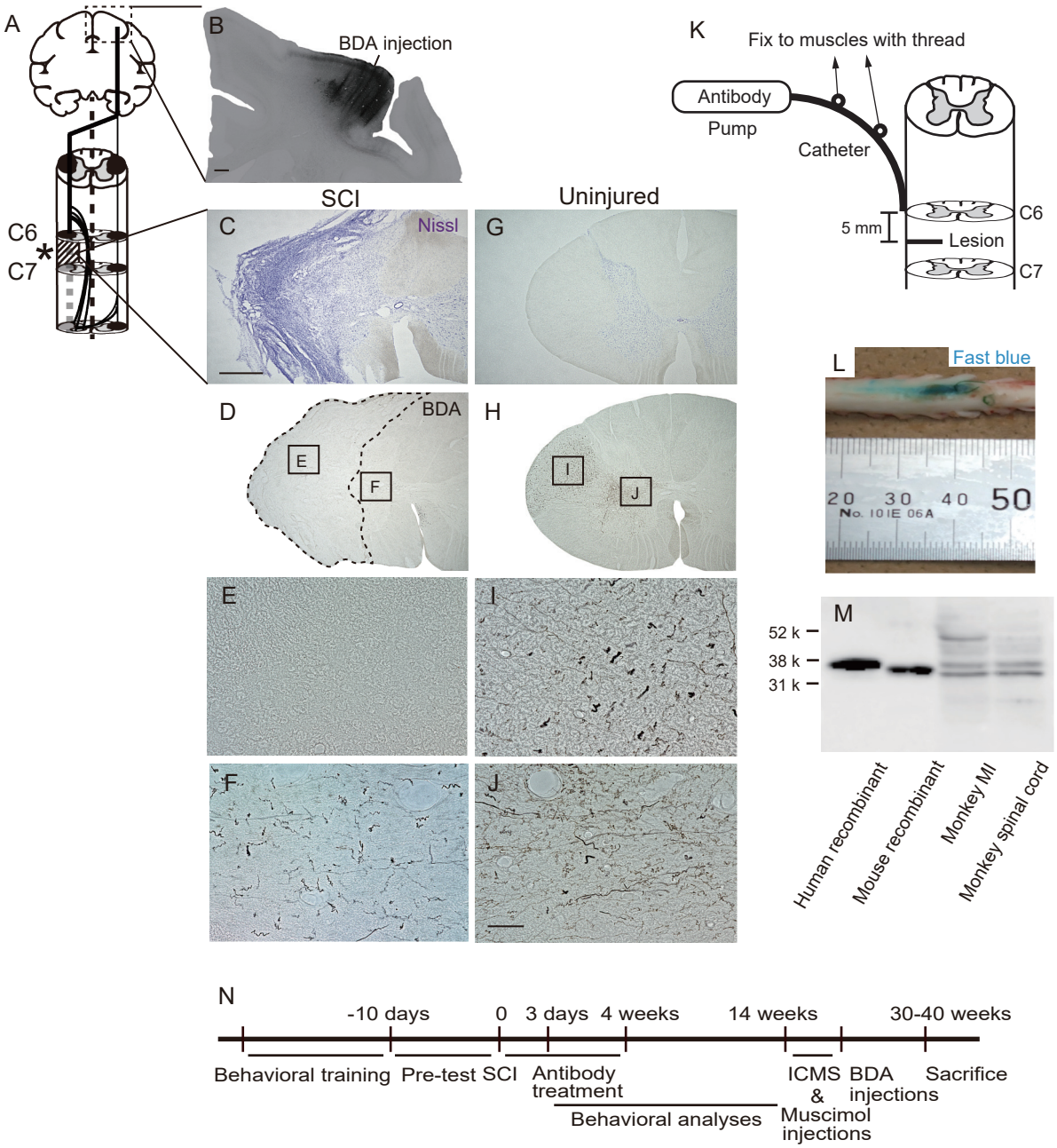

Figure 1
Nakagawa et al.

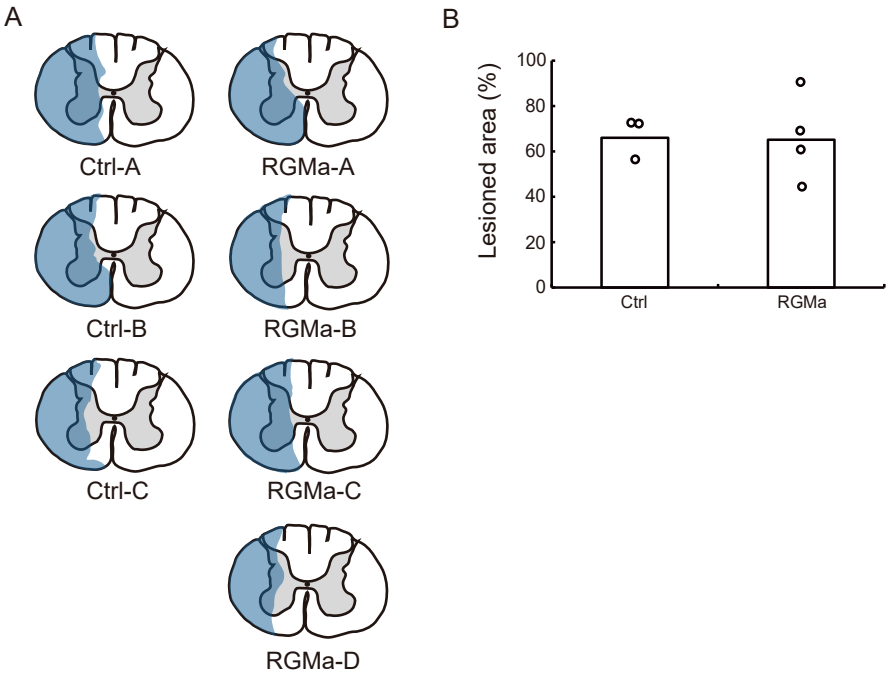

Figure 2

Nakagawa et al.

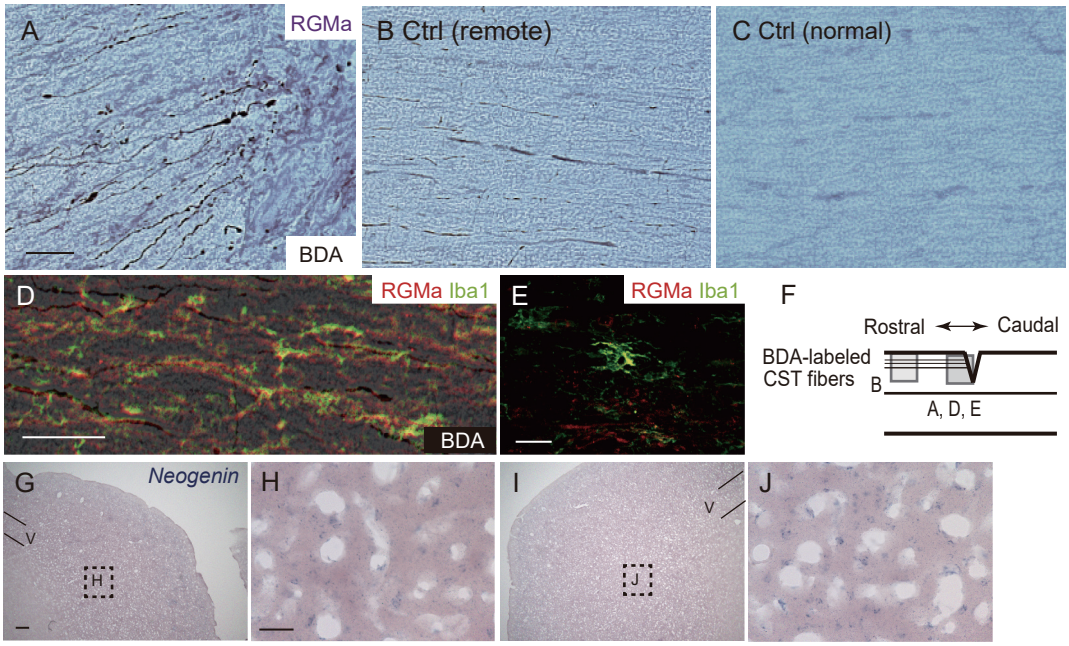

Figure 3

Nakagawa et al.

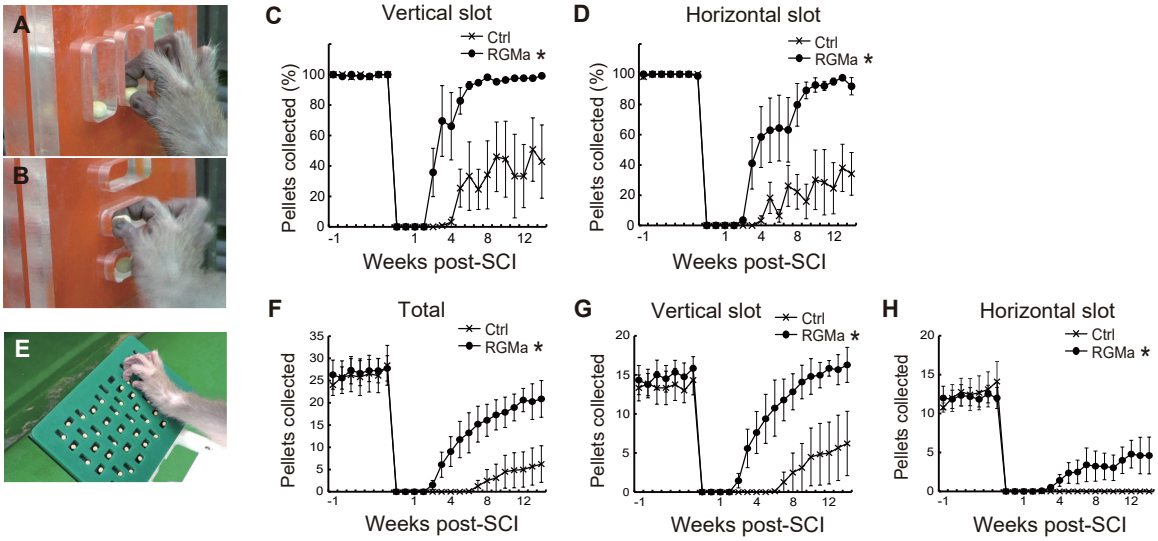

Figure 4
Nakagawa et al.

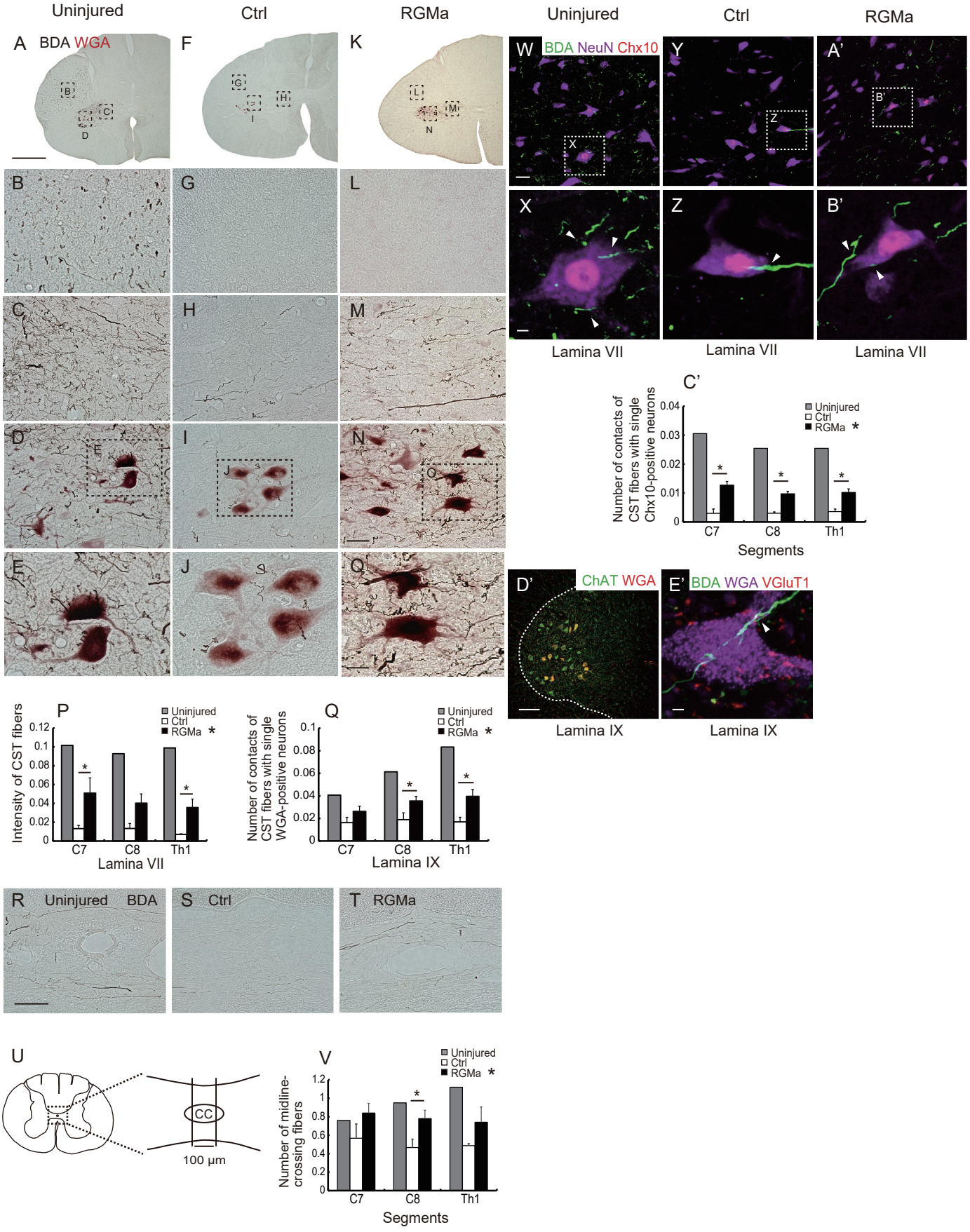

Figure 5
Nakagawa et al.

Supplementary material

Treatment with the neutralizing antibody against repulsive guidance molecule-a promotes recovery from impaired manual dexterity in a primate model of spinal cord injury

Hiroshi Nakagawa[1,2], Taihei Ninomiya[1], Toshihide Yamashita[2], Masahiko Takada[1]

[1]Systems Neuroscience Section, Primate Research Institute, Kyoto University.

[2]Department of Molecular Neuroscience, Graduate School of Medicine, Osaka University.

Video S1. Recovery process of the reaching/grasping task performance in a control antibody-treated and an anti-RGMa antibody-treated monkey. Fourteen weeks after SCI, the control antibody-treated monkey can manage to take out pellets from vertical and horizontal slots mainly using a power grip. On the other hand, the anti-RGMa antibody-treated monkey can take out at least some pellets from both types of the slots skillfully using a precision grip.

Video S2. Recovery process of the modified Brinkman board test performance in a control antibody-treated and an anti-RGMa antibody-treated monkey. This movie shows that the monkeys take out pellets before, 3 days, and 14 weeks after SCI. Before SCI, the monkeys smoothly take out pellets from both the vertical and the horizontal slots. Just after SCI, the monkeys cannot take out any pellet at all. Fourteen weeks after SCI, the control antibody-treated monkey can take out some pellets only from the vertical slots. On the other hand, the anti-RGMa antibody-treated monkey can take out pellets not only from the vertical slots, but also from the horizontal slots.